DECONVOLUTION OF X-RAY BACKSCATTER DIFFRACTION DATA FOR NDE OF CORROSION

Feng Qiu, W. L. Anderson and P. S. Ong
Electrical Engineering Department
University of Houston
Houston, TX 77204-4793

INTRODUCTION

The problem of corrosion of steel surfaces under thermal insulation is one that plagues the petroleum, petrochemical, chemical and pipeline industries [1,2]. Often internal surfaces, as well, are subject to attack by moisture, acids or other corrosive influences. Thermal insulation renders traditional NDE methods mostly ineffective but is essentially transparent to x-rays in the energy ranges commonly used for industrial radiography. Since transmission radiography is severely hampered by the need for access to "both sides" of the object being tested, the use of NDE methods employing Compton backscattered x-rays is strongly suggested [3, 4]. Through appropriate collimation of incident and backscattered x-rays, depth as well as transverse information concerning the object under examination can be resolved. Access is required only to one side of the object, making the method potentially useful for examination of large vessels as well as pipelines.

X-ray backscatter imaging is a possible approach to the pipeline corrosion problem [5, 6], but generally it appears that considerably simpler (i.e., non-imaging) implementations of the backscatter concept will be required for cost-effectiveness. The central problem is to estimate the thickness of the intact steel; this entails finding the boundary between rust and steel at the outer surface and the boundary of the inner surface. A new "transcatter" method (described elsewhere in these reviews) we are exploring will, we believe, obviate the need to locate the inner surface boundary, but still requires resolution of the boundary between insulation and rust.

Sufficient collimation of incident and backscattered x-rays can furnish such resolution under the conditions, first, that there must be enough contrast (i.e., difference in electron density) available between the iron oxide and the steel at the boundary, and secondly, that the number of photon counts at sufficiently closely spaced points within the scan range encompassing this boundary must provide an adequate signal/noise ratio. Data acquisition time of course translates directly to cost, so in considering possible NDE systems in this context one must closely examine the trade-off between scan speed and resolution. Evidently the extent of such tradeoff cannot be determined without knowing the effectiveness of signal processing for deconvolving the data. The purpose of the investigation reported here is to examine various deconvolution possibilities and determine which may be promising in application to NDE of corrosion effects on steel surfaces under thermal insulation.

Our investigation will be based on the assumption that the data at any sample location on the surface are in the form of a profile showing backscatter intensity as a function of depth. A configuration for generating such a profile could consist, for example, of a fixed collimated source aimed at the surface under examination and a movable collimated

Review of Progress in Quantitative Nondestructive Evaluation, Vol. 12
Edited by D.O. Thompson and D.E. Chimenti, Plenum Press, New York, 1993

detector for measuring x-ray flux backscattered from various depths. It is evident that a fundamental problem is the increase of breadth of the point spread function with increasing depth. This adds greatly to the complexity of the deconvolution process. However, as remarked above, our transcatter method will require resolution only of the outer surface region, and we consider it likely that the assumption of a fixed point spread function will be adequate in this limited region. Thus, although our studies are addressed to deconvolution of "complete" sample profiles (both front and back surfaces), the point spread functions used in the algorithms are held constant. Our initial purpose is to sort through the great variety of potentially applicable algorithms to determine which may be most promising for this type of problem. The acquaintance thus gained of their general characteristics should allow narrowing the field to address the specific problem of delineating the boundary on the outer surface between rust and steel.

Our investigation to this point has focused on two basic types of deconvolution algorithms: one uses operations in the Fourier domain, and includes the traditional kinds of filters such as inverse or pseudo-inverse filters, Wiener-type filters, power spectrum equalization filters, and modifications or close relatives of these. The other principal type of deconvolution is iterative, using operations in the spatial domain. Both have advantages and disadvantages. An advantage of Fourier-domain filters is simplicity, ease of use and speed, even though these as well as iterative methods must be implemented digitally for the type of data concerned here. Iterative algorithms, on the other hand, require greater numerical computational power and are relatively time-consuming, but provide considerably greater flexibility.

THEORY

The generally used model, and the one used here for our deconvolution investigations, is:

$$g(x) = h(x) \otimes f(x) + n(x) \tag{1}$$

where $g(x)$ represents the measured data (backscatter intensity vs depth), $h(x)$ is the system point spread function, $f(x)$ is the true signal, and $n(x)$ is the (assumed additive) noise. The symbol "$\otimes$" represents the convolution operation. The goal of deconvolution is to obtain a "best" estimate of $f(x)$. Differences between traditional filtering methods arise on the basis of different interpretations of "best", while differences between iterative algorithms can be based additionally on different choices of implementation of the algorithms. Inevitably, the quality of the estimate in any case is limited by the amplitude and nature of the noise. We consider each of these categories in turn below.

Traditional Filtering Methods

The most fundamental filter in the category is the inverse filter. If noise is zero or negligible, Eq. (1) can be written as $g(x) = h(x) \otimes f(x)$ which in principle can be solved exactly by the use of Fourier transformation, leading to the result

$$f(x) = F^{-1}\left(\frac{G(f)}{H(f)}\right) \tag{2}$$

where $G(f)$ and $H(f)$ are Fourier transforms of g and h respectively. The inverse filter gives a solution that minimizes the mean square error

$$\| g(x) - h(x) \otimes f(x) \|^2. \tag{3}$$

However the solution is singular at zeros of the denominator in Eq. (2), and even if $H(f)$ has no zeros it could be ill-conditioned because of noise or numerical error. Acceptable performance of the inverse filter may be obtained if it is not singular and the noise is negligible, but generally great care must be exercised in its use.

The Wiener filter is based on minimizing the mean square error defined as

$$\|\hat{f}(x) - f(x)\|^2 \tag{4}$$

where $\hat{f}$ is an estimate for f, and can be considered the output of the Wiener filter when the input is g. It can be shown that the Wiener filter estimate in the case of noise uncorrelated with signal is

$$\hat{f}(x) = F^{-1}[W(f)G(f)] \tag{5}$$

where $W(f)$ is the Wiener filter transfer function given by

$$W(f) = \frac{H^*(f)}{|H(f)|^2 + |N(f)|^2/|F(f)|^2} \tag{6}$$

and where $N(f)$ and $F(f)$ are spectra for noise $n(x)$ and signal $f(x)$ respectively. It is easily seen that the Wiener filter is better conditioned than the inverse filter because of the noise/signal ratio term in the denominator of Eq. (6). Evidently it reduces to the inverse filter if the noise is zero.

The power spectrum equalization (PSE) filter is obtained from minimizing the difference between the power spectra of the estimate and signal; i.e., from requiring that

$$|\hat{F}(f)|^2 = |F(f)|^2. \tag{7}$$

The transfer function of the PSE filter is given by

$$W(f) = \left[\frac{1}{|H(f)|^2 + |N(f)|^2/|F(f)|^2}\right]^{1/2}. \tag{8}$$

Implementation of Traditional Filters

Several considerations enter into the implementation of inverse, Wiener and PSE filters. For the inverse filter the major problem is the singular points of $H(f)$. One way to deal with it is to adopt the following form for the inverse filter solution

$$f(x) = F^{-1}\left[\frac{H^*}{|H|^2}\right] \tag{9}$$

and set the result of the division to zero whenever $|H|^2$ is zero or less than some chosen threshold. This solution is called the pseudo-inverse.

In the case of the Wiener filter the power spectra for signal and noise should be known a priori, but in practice we may not know them exactly. It may then be convenient to write the transfer function for the Wiener filter as

$$W(f) = \frac{H^*(f)}{|H(f)|^2 + 1/(SNR)^2} \tag{10}$$

where SNR is an estimated (constant) signal to noise ratio, then examine the outcome for various choices of the constant and select the one that seems to give the best performance. In Eq. (8) the same thing can be done for the implementation of the PSE filter.

Iterative Algorithms

Apparently one of the earliest iterative approaches to deconvolution was by van Cittert, in application to spectroscopic data [7]. The iterations proceeded according to the formula

$$\hat{f}^{k+1} = \hat{f}^k + r(g - h \otimes \hat{f}^k) \tag{11}$$

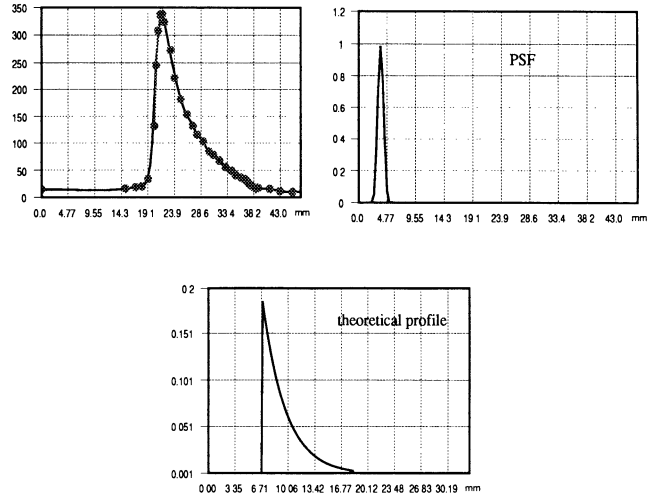

Fig. 1. Experimental data profile, point spread function and theoretical profile.

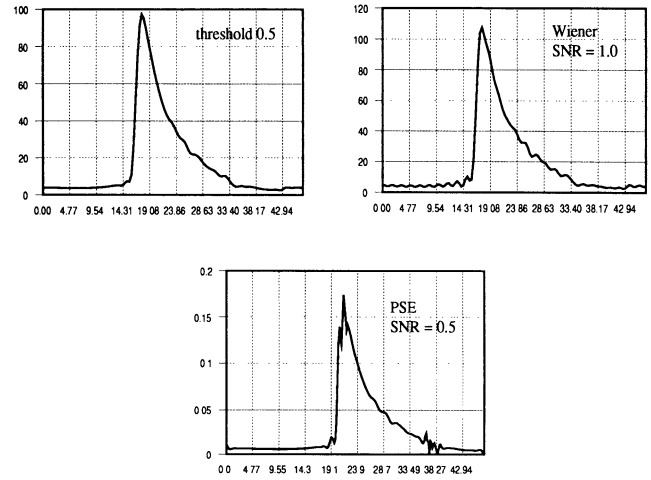

Fig. 2. Results of inverse, Wiener and PSE filtering.

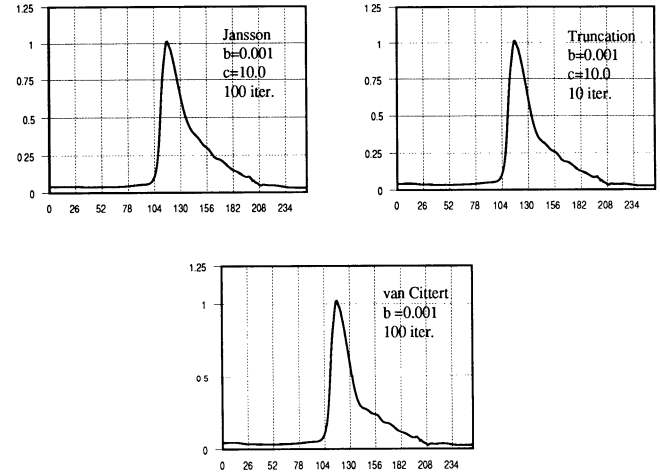

Fig. 3. Results of using Jansson's, truncation and van Cittert's iteration algorithms.

where $\hat{f}^{k+1}$ and $\hat{f}^{k}$ are the (k+1)th and k'th iteration results, respectively, and r is a "selected" constant which determines the step size for iteration. Various modifications to (11) have been reported[8,9], among which are a "truncation" modification, and Jansson's method. Both of these take the same general form as (11) except that r is no longer constant, but a function of the k'th iteration value, i.e., $r = r(\hat{f}^{k})$. For the truncation method r is specified by

$$r(\hat{f}^{k}) = \begin{cases} 0 & \hat{f}^{k} > c;\ \hat{f}^{k} < 0 \\ b & 0 \le \hat{f}^{k} \le c \end{cases} \tag{12}$$

which limits the range of $\hat{f}^{k}$ to $[0, c]$. The value of c must generally be determined by judgment of the nature of the problem or trial and error. In using Jansson's method, r is given by the more elaborate rule

$$r(\hat{f}^{k}) = b\left(1 - \frac{2}{c}\left|\hat{f}^{k} - \frac{c}{2}\right|\right) \tag{13}$$

Here we have assumed that the values of signal are non-negative and do not exceed a certain maximum value c. These limitations are derived from the fact the experimental readings for x-ray detection are x-ray intensities, which can not be negative. The existence of a specific upper limit can be guaranteed by normalization, of course.

An inherent difficulty with deconvolution of x-ray backscatter signals generally is that attenuation rapidly becomes larger with increasing depth. Even if time is taken to accumulate a large number of counts at each point, the presence of background inevitably results in a lower signal/noise ratio at the greater depths. A modification we have introduced to the iteration equation (11) (as also modified to let $r = r(\hat{f}^{k})$) is addressed to this problem. It consists of introducing another constant a in the following manner:

$$\hat{f}^{k+1} = \hat{f}^{k} + r(\hat{f}^{k})\,(a \cdot g - h \otimes \hat{f}^{k}). \tag{14}$$

We choose a to be large enough (by trial and error) to clip the iteration curve so as to compensate for the attenuation.

The algebraic reconstruction technique (ART) [10] is another basic iterative algorithm, and has the form

$$\hat{f}^{k+1} = \hat{f}^{k} + \frac{(\vec{g}_i - \vec{h}^{t}_i \cdot \hat{f}^{k})}{\vec{h}^{t}_i \cdot \vec{h}_i} \cdot \vec{h}_i \tag{15}$$

where $\vec{g}_i$ is the i'th element of the raw data vector $\vec{g} = [g_1\ g_2\ \ldots\ldots g_N]^t$ and $\vec{h}_i$ is the i'th column vector of the matrix for the point spread function $H = [\vec{h}_1\ \vec{h}_2\ \ldots..\ \vec{h}_N]^t$. The iteration starts from an initial guess $\hat{f}^{0}$, which can be chosen as $\vec{g}$, and goes through all the vectors of the H matrix, then starts over again. As can easily be surmised, the fundamental structure of this algorithm makes it slow, but some variations exist [11] which can speed the process. The key point here is that the H matrix has to be consistent; otherwise no unique solution can be found. The final solution is just the solution with least-mean-square error.

DECONVOLUTION RESULTS AND DISCUSSION

Some of the measurements made in our laboratory provided a set of points representing the backscatter profile for a 16.24 mm thick aluminum plate, and points representing a point spread function (PSF) obtained using a thin aluminum sheet. The curves shown in Fig. 1 were obtained using cubic splines fitted to the experimental points; also we show a theoretical profile. It is seen here that the signal/noise ratio is high around the peak of the profile (front surface) and low at the tail, where the depth is larger and attenuation greater. The theoretical curve (no noise) of course shows sharply delineated front and back surfaces with exponential decrease along the depth direction.

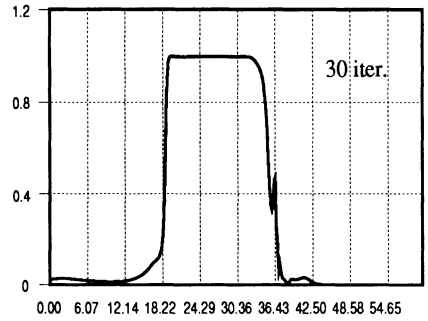

Fig. 4. One result of using our modification of the van Cittert algorithm.

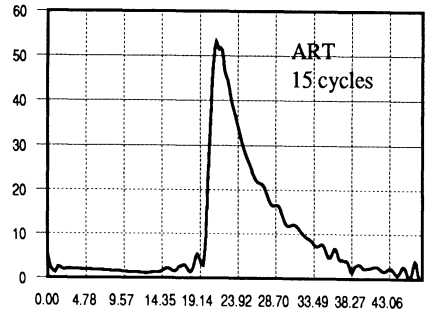

Fig. 5. Results of using the ART algorithm.

Sample results from inverse, Wiener and PSE filtering are shown in Fig. 2. Special consideration, as discussed above, has been given to singularity of the inverse filter and to the signal/noise ratio terms in the Wiener and PSE filters. We see that these three filters give a sharper front edge than the raw profile; also it is obvious that theWiener and PSE filtered results are less subject to oscillation and better conditioned than the inverse filter. For the Wiener and PSE filters the SNR parameter must be chosen carefully to achieve the best results.

Selected results for iterative algorithms (van Cittert, truncation and Jansson) are shown in Fig. 3. We observe that the van Cittert, truncation and Jansson methods give good definition of the front surface, but tend to blur the shoulder associated with the back surface. It seems to be characteristic of these methods that they restore single peaks well, but perform considerably more poorly where details of a more complex type of profile are desired.

In Fig. 5 we see that ART gives better results than the others shown above, but computationally it has the characteristic of diverging very slowly as the iterations continue. This is a result of the fact that the measured data are noisy so the constraints defined by the columns of matrix H in (16) are not consistent. It is interesting to observe, however, that ART provides the possibility of incorporating a point spread function that varies with depth.

CONCLUSIONS

The Fourier domain filters are fast and efficient, and (with care) give generally acceptable results. The algorithms based on van Cittert's iteration equation seem not to be promising for the deconvolution of the entire backscatter profiles but give good front surface definition.

A modification we introduced to van Cittert's equation was found to give apparently good results. Both front and back edges were restored and attenuation compensated, although the choice of the parameter was by trail and error.

These conclusions must, however, be regarded as extremely tentative. A considerably greater variety of data must be subjected to investigation before strong inferences can be drawn. Most of our attention up to now has been directed to establishing computer programs to provide not only efficient computation but prompt graphical displays of results. The greatest usefulness of immediate graphical feedback occurs for the iterative procedures, where often the iterations must be stopped at some "optimum" point, with optimality a matter of judgment of the person running the programs.

Future investigation is to be directed to comparisons between algorithms for a broader variety of data. In that work we will be making use primarily of simulations, with added random noise.

ACKNOWLEDGEMENTS

This work was supported in part by the University of Houston Energy Laboratory and by the Advanced Technology Program of the State of Texas.

REFERENCES

1. Ashbaugh, W. G. and T. F. Laundrie, "A study of corrosion of steel under a variety of thermal insulation materials," *Corrosion of Metals under Thermal Insulation, ASTM STP 880,* W. I. Pollock and J. M. Barnhart, Eds., American Society of Testing and Materials, Philadelphia, pp. 121-131 (1985).
2. Anderson, W. L., B. D. Cook and P. S. Ong, "X-ray Backscatter Diffraction for NDE of Corrosion," Review of Progress in Quantitative NDE, University of California at San Diego, La Jolla, CA, July 15-20, 1990.
3. Harding, G., "On the sensitivity and application possibilities of a novel Compton scatter imaging system," *IEEE Trans. Nuclear Sci.*, vol. NS-29, no. 3, June 1982.
4. Kosanetzky, J., G. Harding, K. H. Fischer and A. Meyer, "Compton back-scatter tomography of low atomic number materials with the COMSCAN system," Technical Information Bulletin, Philips Industrial X-ray Supply Center, Hamburg, 1988.
5. Bossi, R. H., K. D. Friddell and J. M. Nelson, "Backscatter X-ray imaging," *Materials Evaluation*, vol. 46, pp. 1462-1467 (1988).
6. Anderson, W. L., B. D. Cook and P. S. Ong, "X-ray backscatter imaging with the ComScan system", *Paper Summaries, Industrial Computed Tomography II Topical Conference"*, San Diego, CA, May 20-24, 1991, pp 102-105 (American Society for Nondestructive Testing, Inc., Columbus, OH).
7. van Cittert, P. H., "Zum Einfluss der Spaltbreite auf die Intensitatswerteilung in Jansson, P. A., *Deconvolution with Application in Spectroscopy,* New York: Academic, 1984.
9. Crilly, P. B., "A quantitative evaluation of various iterative deconvolution algorithms", *IEEE Trans. Instrum. Meas.*, vol. 40, pp. 558-561, 1991.
10. Gordon, R., R. Bender and G. T. Herman, "Algebraic reconstruction techniques (ART) for three dimensional electron microscopy and X-ray photography", *J. Theor. Biol.*, vol. 29, pp. 471-481, 1970.
11. Andersen, A. H. and A. C. Kak, "Simultaneous algebraic reconstruction technique (SART): a new implementation of the ART algorithm," *Ultrason. Imaging,* vol. 6, pp. 81-94, 1984.